Asociación Argentina
de Mecánica Computacional

Mecánica Computacional Vol XL, págs. 433-442 (artículo completo)
F.A. Avid, L.C. Bessone, P. Gamazo, J.J. Penco, M.A. Pucheta, M.A. Storti (Eds.)
Concordia, 6-9 Noviembre 2023

PREDICTION OF THE CHARACTERISTIC PRESSURE PULSATIONS IN A REVERSIBLE PUMP-TURBINE

Alfred Fontanals[a], Alfredo Guardo[a] Miguel G. Coussirat[b] , Flavio H. Moll[b], Eduard Egusquiza[a] y Germán L. Martínez[b]

[a]*Centre de Diagnòstic Industrial i Fluidodinàmica, Universitat Politècnica de Catalunya (UPC), Av. Diagonal, 647, 08028 Barcelona, España. https://cdif.upc.edu/en*
[b]*Laboratorio Modelado Aeroplasticidad (LAMA), Dpto. Electromecánica FRM, Universidad Tecnológica Nacional, Coronel Rodríguez 273, 5500 Mendoza, Argentina, miguel.coussirat@frm.utn.edu.ar, https://www4.frm.utn.edu.ar*

Keywords: Rotor-stator interaction, Turbulence, Pressure pulsation, Computational Fluid Dynamics, Reversible pump-turbine.

Abstract: Reversible Pump- Turbine turbomachines are frequently used in peaking load hydroelectrical power plants. These plants contribute to satisfy the energy demand during peak load periods. Its dynamic behaviour is influenced by the flow structures developed along the distributor and runner vanes. This behaviour depends both on the internal design of the machine and its operating conditions, whether it works as pump or as a turbine. High-amplitude pressure pulsations appear due to the rotor-stator interaction phenomenon, and under certain operating conditions, the frequency of these pulses can seriously affect the structural integrity of the machine. The goal of this study is to assess the dynamic behaviour of a low-specific-speed reversible pump-turbine when working both as a turbine or as a pump. For validation, the obtained numerical results for the pressure pulsation in both operating modes are compared to experimental results measured on a working prototype. These results could be useful to enhance the knowledge concerning the behaviour of the pressure pulsations due to the internal flow dynamics into the machine.

1. INTRODUCTION

The need for storage in electricity systems is increasing because large amounts of variable solar and wind generation capacity are being deployed. About two thirds of net global annual power capacity additions are solar and wind. It is known that pumped storage combined with thermal generating capacity allows thermal units to operate at nearly constant output and best efficiency (BE), Stelzer and Walters, 1977, De Siervo et al., 1980, Raabe 1985, Valero et al. 2017, Blakers et al. 2021, Zhao et al., 2022. Because of its ability to store energy efficiently and to reach the operations conditions quickly (e.g., for a pumped storage plant, it can assume full output load in some minutes compared to the half hour required for a steam plant to achieve maximum output from spinning reserve) pumped storage also could play a fundamental role in the current energy transition towards solar and wind energies, helping advance the deployment of renewable energies while helping to maintain the stability of the electrical grid. Reversible Pump-Turbines convert the energy surplus during low electricity demand hours into potential hydraulic energy by pumping water to a higher reservoir. The stored energy can be converted back into electricity when required, by operating the machine runner in turbine mode. Due to new regulation requirements, machines must extend their operating range to match energy generation with consumption for the grid stability, Valero et al. 2017.

The Reversible Pump-Turbine (RPT) machine, Fig.1, has many unique features (e.g., fewer blades and higher rotating speed than a regular reaction turbine, i.e., a Francis turbine). RTP is a complex structure formed by a mixed-flow impeller attached to a rotor and rotating inside a casing full of water with very small clearances between the rotating and the stationary parts. The difference in operating parameters is also noticeable, as they operate with high water heads, leading to a much larger hydraulic forces generated within the RPT, Stelzer and Walters, 1977, Raabe 1985, Egusquiza et al., 2016, Johansen 2021. Furthermore, the blade load uses to be larger if compared with a Francis turbine which is equipped with at least twice the number of blades for equivalent flow rate and head, Mateos et al., 2006.

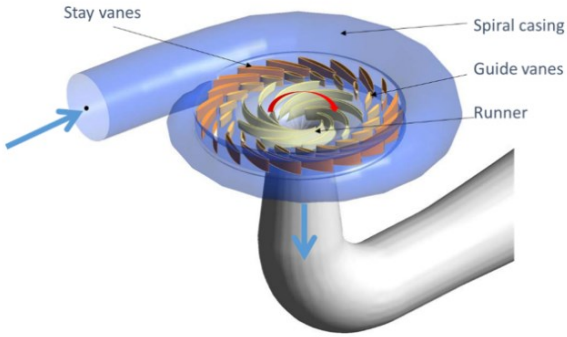

Fig.1. Reversible Turbine-Pump characteristics, Guardo et al., 2021.

For designing a suitable RPT, it is necessary to harmonize the mutually contradictory pump and turbine operation modes, aiming to obtain the maximum mean efficiency. This can only be achieved by knowing the complete diagram of the characteristics for the machine, which is usually not available during the preliminary design, Stelzer and Walters, 1977, De Siervo et al., 1980, Johansen 2021, Zhao et al., 2022.

Several uncertainties appear when the dynamic response of this type of structures is assess, because it is complex and it is very much affected by the rotor-stator interaction (RSI) as well as by the water added mass and the boundary conditions, Egusquiza et al., 2016. In most cases, there are prominent hydraulic forces over the RPT (especially over the impeller), leading to strong instabilities in its behavior. Abnormal hydraulic forces may seriously affect the safe operations of

the machine. Frequently, RPT operations experience great instability issues, leading to start up failure, significant pressure fluctuations and severe vibration of the whole system, Egusquiza et al., 2016, Zhang et al., 2017, Zhang et al., 2021.

RPTs are a type of turbomachine very prone to suffer from RSI since the gap between the stator guide vanes and the runner blades is usually narrow. The highest-level fluctuations in large RPTs are usually originated from RSI in the vaneless region. Pressure pulsations induced by RSI are one of the major sources of excitation resulting in severe vibrations of RPT machines and powerhouses. Hence, the studies of the RSI phenomenon and corresponding transient effects are significantly important to reduce the pressure fluctuations. Many articles have been focused mainly on the RSI mechanism by methods of theoretical analysis, fluid-structure calculation, and model test verification. More recently, numerical tools are added for a more detailed RTP study/design. Zhang et al., 2021, showed that the vaneless area pressure pulsations into the RPT machine, although being within the acceptance criteria during the original design, could possibly be reduced with a more modern design. It was demonstrated that a vaneless space enlargement reduces the RSI induced pressure pulsation. It was highlighted that although the efficiency of a modified design of the runner decreases slightly, pressure pulsations in the vaneless area decrease significantly too.

Other of the physical origins of the RPTs operation instability is the rotating stall phenomenon generated at off-design conditions in generating mode. Recent studies on the rotating stall of RPT are critically reviewed with a focus on the RPT generating mode, e.g., see Zhang et al., 2017, Li J. et al., 2018, Lu et al., 2023. In RPTs the rotating stall initiates at runaway and it is fully developed at a low discharge condition, with a characteristic rotating frequency around of the 50–70% of the impeller rotational frequency. Notorious effects induced by rotating stall include generation of large pressure fluctuations, channel blockage, and strong backflow, all of which contribute significantly to the machine instability. One of the difficulties of studying the hydraulic force on the impeller of a RPT is the presence of a great number of influential factors on these issues (e.g., the working states, the guide vane openings, and the turbine geometries). For example, in the generating mode, RPT could pass three working zones: the turbine zone, the turbine brake zone and the reverse pump zone, which are separated by the runaway line and the zero-flow-rate line. A similar behavior can be seen in pumping mode.

To avoid this operational instability, an improvement of RPT machines performance is necessary. The influence of water head variations on the performance of several RTP prototypes was experimentally studied in generating/pumping mode within a wide range of load conditions, (e.g., see the classical database from De Siervo et al., 1980). More recently, several experimental research was focused on effects of the pressure fluctuations within the runner/impeller at different water heads. Furthermore, effects of monitoring points and load variations on the induced unstable behavior (e.g. blade passing frequency and its harmonics) were quantitatively studied, reveling that water head variations play a significant role on the pressure fluctuations and their propagation mechanisms inside the RPT, e.g., see Guedes et al., 2002, Rodriguez et al., 2014, Li J. et al., 2018, Lu et al., 2023.

Turbomachinery initial design is mainly based on the assumptions that the flow is steady in the distributor, runner, and diffuser. This approach is suitable for the classical turbomachines design allowing to obtain an initial design of the runner and the distributor. However, to design real and more compact machines, with a wide operating range, and for the refurbishment of hydraulic devices, it is necessary to consider the unsteadiness of the flow to know in detail the unsteady phenomena inside the machine.

Numerical tools, i.e., Computational Fluid Dynamics (CFD), allow to improve our knowledge related to the RPTs flow unsteadiness. To validate/calibrate the CFD design technique, the experimental data are of prime importance. CFD as a modelling tool has been extensively validated in hydraulic turbine applications, Trivedi et al., 2016. The turbomachinery optimization is

nowadays based on CFD simulation of internal flow and, in practice, the coupling between different parts of the machine could be considered. Several numerical techniques are now available to compute these flows and to assess the machine dynamic response. The validation of these methods becomes essential, and is only possible with detailed experiments on working prototypes, notably to define the validity range of this kind of calculation, Ciocan et al., 2000, Guedes et al., 2002, Li J. et al., 2016 and Li J. et al., 2017, Guardo et al., 2021. The works from Guedes et al., 2002 and Li D. et al., 2017 deal with unsteady CFD computations using sliding/dynamics mesh formulations and turbulence modeling for unsteady flow in RPT under different operation conditions and for different RPT machines. The obtained results indicate that the numerical model is capable of accurately reproduce the features of the incompressible flow encountered in RTP for nominal and off-design operation conditions. It is also shown that the unsteady flow computations are very demanding in mesh refinement if small scales flow structures must cross the sliding mesh interface. Then, it was demonstrated that a CFD analysis could be very useful to identify instabilities related to the RSI phenomenon in RPT machines. It is also possible to compare results against theoretical tools (e.g., see Rodriguez et al., 2007). The comparison including performance and pressure characteristics between numerical, theoretical, and experimental results shows a good agreement.

It was highlighted that the hydraulic force on the RTP might cause serious problems (e.g., the abnormal stops due to large vibrations of the machine), affecting the safe operations of the pumped energy storage power plants. Li J. et al., 2017, demonstrated that both the amplitude of the hydraulic force and its dominant components strongly depend on the operating conditions and the guide vane openings. For example, the axial force parallel with the shaft is prominent in the turbine mode while the force perpendicular to the shaft is the dominant near the runaway and the turbine brake modes. The physical origins of the hydraulic force are further revealed by the analysis of the fluid states inside the impeller.

Therefore, it is possible to say that to increasing the CFD expertise related to the RSI phenomenon in turbomachines, clearly could be of paramount importance when a new RPT machine will be designed saving time and costs, because the experimental option is very expensive.

2. METHODOLOGY

A geometrically similar scaled model of the RPT prototype studied in Egusquiza et al., 2011, was defined for this CFD study. This work focuses on the RSI phenomenon when the RPT operates both in mode pump and mode turbine. Details of the RPT prototype can be found in Egusquiza et al., 2011 and Guardo et al., 2021. The scaled model consisted of a runner with diameter D= 510 mm and z_b=7 blades, and a distributor with z_v=16 guide and stay vanes, rotating at 3,435 rpm, maintaining the prototype dimensionless specific speed n_s=0.70. RSI characteristic frequencies for turbomachinery can be obtained for the rotor blade by computing $f_b = n\, z_b\, f_f$ and $f_f = (rpm/60)$; being n an arbitrary, positive integer used to represent the harmonics and f_f the runner rotation frequency, see details in Guardo et al., 2021. The characteristic RSI wave is composed by several harmonics computed by the classic theory, Rodriguez et al., 2007 and some of they are reported in Table.1 for f_f=57.25 Hz, related to the *rpm* value.

n	1	2	3	4	5
f_b (Hz)	400,8	801,5	1202,3	1603,0	2003,8

Table.1: Computed characteristic pulse frequencies in the stator.

2.1. Numerical setup

Computational models for the studied cases were generated using a sliding mesh technique, Mathur, 1994. The computational domain studied consisted of three control volumes (distributor, runner, and draft tube) linked by numerical interfaces (Fig.2). Tetrahedral meshes were created for both the RPT model runner and distributor Mesh independency was tested by means of steady-state simulations, determining pressure drops through rotor and distributor control volumes for best efficiency point (BEP) (0.953m^3/s flow rate, obtained through similarity analysis of the prototype's BEP) operating conditions, see complete details in Guardo et al., 2021.

The tested mesh element sizes ranged from 3 to 10mm. Mesh independency was achieved at around 4.9e+6 elements for the rotor, and 4.3e+6 elements for the distributor, corresponding to average element sizes of 6mm and 5mm, respectively.

A boundary layer mesh, with 60 <y^+< 300, was attached to both distributor vanes and rotor blades, and an elbow-type draft tube with varying cross-sections with a 0.34e+6 elements hexahedral mesh was included in the computational model. The addition of a draft tube improves the runner pressure results in turbine CFD models by allowing pressure recovery downstream.

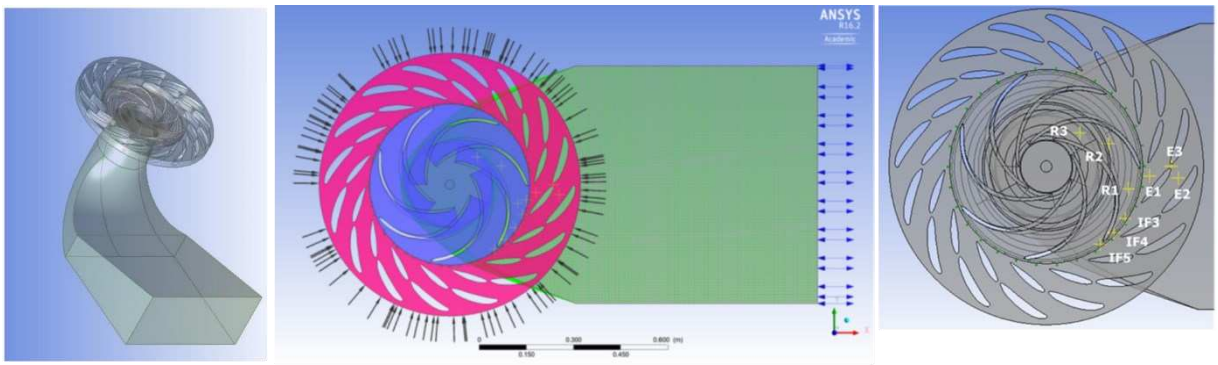

Fig.2. Geometry, Boundary conditions and location of the pressure monitoring points (E1, E2 and E3).

Unsteady-state numerical simulations for the of the RPT model working at the BEP were carried out using Ansys® CFX v16.2 CFD software, Ansys 2020. The boundary conditions imposed consisted of the rotor rotational speed (3,435rpm), mass flow rate (953kg/s) and flow direction (parallel to the guide vane chord) at the distributor inlet and a reference pressure at the draft tube outlet. The time step selected for the unsteady analysis corresponded to a 1° rotation of the runner, Simpsom et al., 2009. A high-resolution advection scheme (which consists of a numerical advection scheme with a calculated blending factor) was selected for the stabilization of the convective term. Time discretization was achieved by a 2ndorder backward Euler scheme. Tri-linear finite element-based functions were used as an interpolation scheme. A coupled solver for velocity components and pressure as a single system was set, including a linearization of the non-linear equations (coefficient iteration), and then, these equations were solved by an algebraic multigrid (AMG) solver. For convergence criteria, residual types were set to the root mean square (RMS) value of the normalized residuals with a target value of 1×10^{-3}. Simulations were carried out on a 64-bit, Intel core i7 processor (6 core|12 thread) @ 3.3GHz and 32GB RAM, with simulation times of about 60 to 110h (depending on the studied case) to reach quasi-steady flow conditions in all regions of the model.

The SST k–ω turbulence model was used to compute the turbulent flow quantities. The SST k–ω model belongs the so-called 'Two-Equation EVM models' group, being this model a modification of the Wilcox Standard k-ω model, where the selected variables for turbulence scaling are the turbulence kinetic energy k and the specific rate of dissipation ω, instead of the rate

of dissipation of turbulent kinetic energy ε used in the k-ε models' family, Menter, 1994, Menter et al., 2005, Versteeg et al., 2007. For this model, a turbulence intensity of 5% was used as a boundary condition at the stator inlet.

2.2. CFD Results post-processing

Pressure fluctuations within the RPT CFD model were recorded for pump and turbine operating modes to characterize the RSI effect. Pressure monitoring points were added to the rotor (R1, R2 and R3), distributor (E1, E2 and E3) and radial gap (IF3, IF4 and IF5) of the RTP model to capture the unsteady pressure pulsations, see Fig.2. The recorded temporal pressure signals were processed using a Fast Fourier Transform (FFT) algorithm, Ansys 2020. These signals consisted of 0.5s of flow time, recorded once the computational model reached quasi-steady state (i.e., when the oscillating pressure signal period and amplitude have been stabilized). This quasi-steady state was reached after 20 to 30 runner revolutions, depending on the studied case. Sampling frequency was set to 20,610Hz for all cases, resulting in a 2.0Hz frequency resolution for the frequency spectra obtained. These spectra were analyzed to complement the information extracted from the recorded pressure data.

2.3. Experimental database used for CFD validations

The numerical results obtained from the CFD model were compared against experimental data obtained on a working RTP prototype. A schematic representation of the RTP prototype is shown in Fig.3. The RTP prototype was designed for a net head of 376m and a volumetric flow rate of 32m^3/s, and its rotating speed of the pump turbine unit is 600rpm, the runner has a diameter of 2.87m and its nominal power is about 100MW.

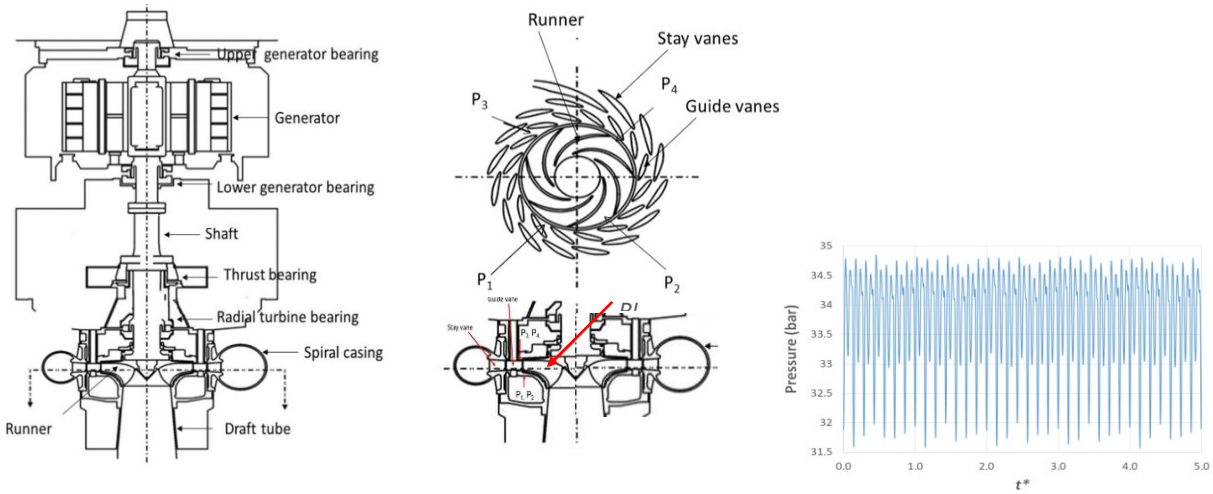

Fig.3. Left: General configuration of the RTP prototype. **Middle:** Location of the pressure transducers installed for the experimental study from Rodriguez et al., 2014. **Right:** Example of an RSI pressure signal recorded at location P1 for Best Efficiency Point (BEP), mode turbine, plotted vs. normalized time t^* (using the time of one revolution of the runner as a reference value).

Experimental measurements on the RPT prototype were carried out by members of the CDIF/ETSEIB UPC research group, (e.g., see details in Mateos et al., 2006 and Rodriguez et al., 2014). For these experimental tests, four pressure transducers were installed at different locations of the prototype's head cover. These locations are shown in Fig.3. Wika S-10 pressure transducers were used for the experimental measurements. The transducers' sensitivity is 0.2mV/bar (±5%), and their frequency range is 0–1000Hz (±10%). The pressure signals registered by these

transducers were conditioned using a 16-channel conditioner, Bruel & Kjær model 2694, and recorded with a Sony PC216Ax data recorder with 16bits of resolution and a frequency range of 0–20,000Hz (±10%). Additional details on the experiments and the obtained results can be found in Rodriguez et al., 2014.

3. RESULTS OBTAINED AND DISCUSSION

The pressure signals obtained at the distributor for the prototype and the CFD RPT were postprocessed and reported by means of a defined non- dimensional characteristic pressure coefficient pressure, i.e., $C_p=\rho^{-1}(\Omega D)^{-2}\Delta p$, where: ρ [kg/m^3], is the water density; Ω [rad/s], is the rotational speed; D [m], is the runner exterior diameter; Δp [Pa], is the measured/computed local p, referred to the outlet pressure p_∞ [Pa]. The comparisons between experimental and CFD signals are shown in Fig.4. As it can be seen, the CFD model is able to reproduce the oscillating nature of the pressure pulse in the machine distributor both under mode pump and mode turbine operation.

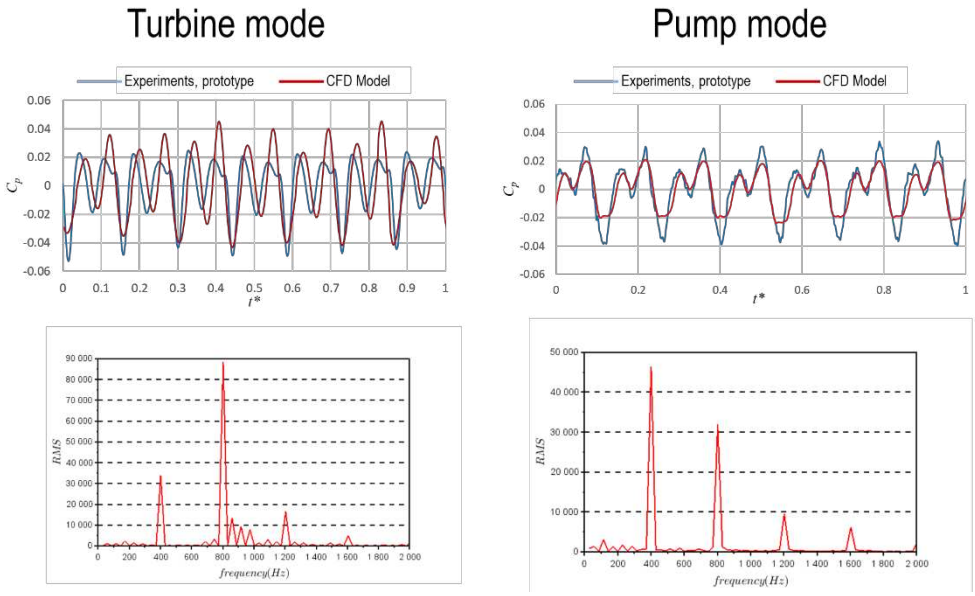

Fig.4. Above: Experimental and CFD results comparisons. Time-based representation for the pressure coefficient (C_p, [Ad]). Notation: t^*, non-dimensional time, Mateos et al., 2006. **Below**: CFD results. Frequency-based representation for the Δp amplitude [Pa] vs characteristic pressure pulsation frequencies.

The computational results capture both the frequency and the amplitude of the pressure pulse with enough accuracy when compared against the experimental data, Fig.4, obtaining an initial validating the numerical model proposed. The differences observed between the experimental and the CFD dimensionless pressure signals can be attributed to the geometric simplifications used in the CFD model, which did not include the machine volute or the breakwater.

Comparisons between the experimental pulsation frequencies, see Table.1, and the ones obtained by CFD, Fig.4, show that these values are well represented by the numerical simulations. Mateos et al., 2006 reported that for turbine mode and lower loads, the first harmonic of the blade passing frequency (f_b) dominates the spectra, but when the load is increasing till the BEP, the second harmonic rises progressively while f_b drops. The CFD results also show this trend, see Fig.4.

4. CONCLUSIONS

A numerical model of a reversible pump-turbine (RPT) was built and used to assess its dynamic behavior by using a commercial CFD code. The Rotor Stator Interaction (RSI) phenomenon was captured, and for that the pressure fluctuations in certain locations of the model were computed for pump and turbine operating modes. The amplitude and characteristic frequencies of the RSI pulsations were computed and compared against experimental measurements obtained from an operating RPT prototype, showing general good agreement. The obtained results showed that the pressure fluctuation in turbine mode is larger than in pumping mode. The frequency computed in both modes also are different, being the main frequency in turbine mode is f_b=801,5 Hz and in pump mode is f_b=400,8 Hz.

Despite that a simplified geometry was used for the CFD modelling, a general good agreement is observed both in the frequency and amplitudes of the pulsations. Some discrepancies were observed in the pressure coefficient (C_p) amplitude values and wave shape when they are compared against the experiments. The main reason of this disagreement could be related to boundary conditions used at the Fink distributor inlet due to not consider the volute influence. More work will be done to improve the machine model geometry and to check the volute effects and compare accuracy of the results versus the rising of the computational cost.

ACKNOWLEDGEMENTS

This current work was partially supported by the Universidad Tecnológica Nacional within its own research programme (UTN/SCTyP, research project AMTCAME0008441TC), by the EEBE, and CDIF/ETSEIB research programmes, all from the Universidad Politécnica de Cataluña (UPC) and by the Fundación Carolina from Spain.

REFERENCES

Ansys/CFX/Fluent Software, 2020-23, http://www.ansys.com/Industries.

Blakers A., Stocks M., Lu B., Cheng C., A review of pumped hydro energy storage, *Prog. Energy,* 3:022003, 2021, doi.org/10.1088/2516-1083/abeb5b.

Ciocan G., Avellan F., Kueny J., Optical measurement techniques for experimental analysis of hydraulic turbines rotor-stator interaction, *Proc.ASME2000/FEDSM'2000 Fluids.Eng.Division Summer Meeting June* 11-15, 2000.

De Siervo F., Lugaresi, A., Modern Trends Selecting Designing Reversible Francis Pump Turbine, *Water Power & Dam Construction*, 32(5):33-42, 1980.

Egusquiza E., Valero C., Estévez A., Guardo A.; Coussirat, M., Failures due to ingested bodies in hydraulic turbines. *Eng.Fail.Anal.*18:464–473, 2011, doi.org/10.1016/j.engfailanal.2010.09.039.

Egusquiza, E., Valero, C., Presas, A., Huang, X., Guardo, A., Seidel, U.; Analysis of the dynamic response of pump-turbine impellers. Influence of the rotor. *Mech. Syst. and Signal Processing*, 68: 330-341, 2016.

Johansen D., Efficiency improvement of Reversible Pump Turbine operation due to implementation of a booster pump, *Msc.Thesis*, NTNU, 2021.

Li D., Gong R., Wang H., Wei Z., Liu Z., Qin D.; Analysis of Rotor-Stator Interaction in Turbine Mode of a Pump-Turbine Model, *Journal of Applied Fluid Mechanics*, 9(5):2559-2568, 2016, doi.org/10.18869/acadpub.jafm.68.236.25086.

Guardo A., Fontanals A., Egusquiza M., Valero C., Egusquiza E.; Characterization of the effects of ingested bodies on the rotor–stator interaction of hydraulic turbines. *Energies,* 14(20), 2021. https://doi.org/10.3390/en14206669.

Guedes A., Kueny J., Ciocan D., Avellan F.; Unsteady rotor-stator analysis of a hydraulic pump-turbine – CFD and experimental approach, *Proc.Hydr.Mach. and Syst*., *21st IAHR Symp*., 2002,

Li J., Zhang Y., Liu K., Xian H., Yu J.; Numerical simulation of hydraulic force on the impeller of reversible pump turbines in generating mode, *Journal of Hydrodynamics,* 29(4):603-609, 2017, doi.org/10.1016/S1001-6058(16)60773-4.
Li D., Wang H, Li Z, Torbjørn K., Goyal R, Wei X, Qin D.; Transient characteristics during the closure of guide vanes in a pump-turbine in pump mode, *Renewable Energy*, 2017, doi.org/10.1016/j.renene.2017.10.088.
Li J., Zhang Y., Yu J.; Experimental investigations of a prototype reversible pump turbine in generating mode with water head variations. *Sci. China Tech. Sci*, 61, 2018, doi.org/10.1007/s11431-017-9169-7.
Lu, J., Yan, W., Tao, R., Wang, Z., Zhu, D.; Exploring the Mechanism of Strong-Pressure Fluctuation under Partial Load in the Turbine Mode of Pump Turbines for Hydro and Marine Power Storage. *Jour. Marine. Scie. and Engineering*, 11(5):1089, 2023. doi.org/ /10.3390/jmse11051089.
Mateos B., Egusquiza E., Escaler X., Coussirat M.; Analysis of Rotor-Stator Interaction excitation and vibration response for Pump-Turbine prototype. *IAHR Int. Meeting of WG on Cavitation and Dynamic Problems in Hydraulic Machinery and Systems*, Barcelona, 28-30, 2006.
Mathur, S.; Unsteady flow simulations using unstructured sliding meshes. *Fluid Dynamics Conference AIAA*, (p. 2333), Reston, VA, USA, 1994, doi.org/10.2514/6.1994-233.
Menter F.; Two Equations Eddy-Viscosity Turb. Models for Eng. Appl., *AIAA J*., 32(8), 1994.
Menter F and Egorov Y.; A scale adaptive simulation model using two-equation models. *43rd AIAA aerospace sciences meeting and exhibit* (p. 1095), 2005.
Menter, F., and Egorov, Y.; The Scale-Adaptive Simulation Method for Unsteady Turbulent Flow Predictions—Part 1: Theory and Model Description, *Flow Turb. Combust*., 85(1), 2010.
Raabe, J.; *Hydro power. The design, use, and function of hydromechanical, hydraulic and electrical equipment*, VDI-Verlag GmbH, 1985.
Rodriguez, C.G.; Egusquiza, E.; Santos, I.; Frequencies in the vibration induced by the rotor stator interaction in a centrifugal pump turbine. *JFE*, 129:1428–1435, 2007, doi.org/10.1115/1.2786489.
Rodríguez, C., Mateos-Prieto, B., Egusquiza, E.; Monitoring of rotor-stator interaction in pump-turbine using vibrations measured with on-board sensors rotating with shaft. *Shock Vibr.*, 2014, doi.org/10.1155/2014/276796.
Simpson, A.T.; Spence, S.W.T.; Watterson, J.K.; A comparison of the flow structures and losses within vaned and vaneless stators for radial turbines. *Journ.Turbomach*., 131, 031010, 2009, doi.org/10.1115/1.2988493.
Stelzer R., Walters R.; Estimating Reversible Pump-Turbine Characteristics, *Technical Report, Engineering and Research Center Bureau of Reclamation*, Denver, 1977.
Trivedi, C.; Cervantes, M.J.; Dahlhaug, O.G.; Numerical techniques applied to hydraulic turbines: A perspective review. *Appl.Mech. Rev*., 68, 010802, 2016, doi.org/10.1115/1.4032681.
Valero, C., Egusquiza, M., Egusquiza, E., Presas, A., Valentin, D., Bossio, M.; Extension of operating range in pump-turbines. Influence of head and load. *Energies*, 10(12), 2017.
Versteeg H. and Malalasekera W., *An Introduction to Computational Fluid Dynamics: The Finite Volume Method*, 2nd Ed., Upper Saddle River, NJ, USA, Pearson Prentice Hall; 2007.
Zhang Y., Zhang Y., Wu Y.; A review of rotating stall in reversible pump turbine [J]. *Proceedings of the Institution of Mechanical Engineers, Part C: Journal of Mechanical Engineering Science*, 231(7):1181-1204, 2017.
Zhang, F., Lowys, P. Y., Houdeline, J. B., Guo, X. D., Hong, P., & Laurant, Y.; Pump-turbine rotor-stator interaction induced vibration: Problem resolution and experience. *IOP Conference Series: Earth and Environmental Science* 774(1), 2021.
Zhao, J. F., Oh, U. J., Park, J. C., Park, E. S., Im, H. B., Lee, K. Y., Choi, J. S.; A review of world-wide advanced pumped storage hydropower technologies. *IFAC-PapersOnLine*, 55(9):170-174, 2022, doi.org/10.1016/j.ifacol.2022.07.030.